Journal of Crystal Growth 61 (1983) 606–614
North-Holland Publishing Company

HYDROGEN URANYL ARSENATE HYDRATE SINGLE CRYSTALS: $H_2(UO_2)_2(AsO_4)_2 \cdot 8H_2O$; GEL GROWTH AND CHARACTERIZATION

E. MANGHI and G. POLLA

División Física del Sólido, Departamento de Física, Comisión Nacional de Energía Atómica, Avda. del Libertador 8250, 1429 Buenos Aires, Argentina

Received 13 September 1982; manuscript received in final form 15 November 1982

Single crystals of hydrogen uranyl arsenate hydrate (HUAsH) were grown in tetramethoxysilane gels at different temperatures, below and above the paraelastic–ferroelastic transition temperature, T_0. The crystals were characterized by X-ray diffraction, chemical etching, scanning electron microscopy and optical microscopy. The habit of the gel grown crystals allowed the three-dimensional features of the domain structure to be studied for the first time. A correlation was made between crystal perfection, domain structure and growth history.

1. Introduction

Troegerite, $H_2(UO_2)_2(AsO_4)_2 \cdot 8H_2O$, is a mineral belonging to the metatorbernite group which can be represented by the formula $A^{z+}(UO_2XO_4)_z \cdot nH_2O$, where A may be almost any monovalent or divalent cation and X = P or As. Previous research [1] had been done on synthetic crystals of troegerite (HUAsH) prepared from solution by cooling from 100°C to room temperature [2]. The mica-like platelets obtained were studied by X-ray diffraction, optical microscopy (OM) and differential scanning calorimetry (DSC): two phase-transitions were found and the domain structure of the ferroelastic phase was described [3–5].

Two problems were still unsolved in this material:

(1) Domain structure on faces other than (001) was not known, because of the mica-like habit of the plates.

(2) It had not been possible to detect by X-ray diffraction (precession method) any differences between the tetragonal (phase I) and monoclinic (phase II) axes contained in the (001) plane.

Thicker crystals were necessary to solve these problems; so we grew HUAsH crystals by the gel method, which is well adapted for growing single crystals of sparingly soluble materials [6,7].

In this study the morphology and characterization of gel-grown single crystals of HUAsH are described.

As-grown crystals as well as cleaved (001) slices were characterized by X-ray diffraction, chemical etching, scanning electron microscopy (SEM) and optical microscopy.

2. Experimental

The chosen growth medium was tetramethoxysilane (TMS) [8,9] which allows one to obtain gelled solutions of arsenic acid. When this solution gellified in the test tubes an aqueous solution of uranyl nitrate was carefully poured over the gel.

By diffusion of both reactants near room temperature the following reaction takes place:

$$2\,H_3AsO_4 + 2\,UO_2(NO_3)_2 \xrightarrow[aq]{TMS} (UO_2)_2H_2(AsO_4)_2 \cdot 8\,H_2O + 4\,HNO_3.$$

The gel forming agent TMS acts only as a support for the diffusion, limiting nucleation and allowing the free growth of the crystal in all directions [6]. Several concentrations between 4 and 10 vol% of TMS were tried. Nucleation density was

0022-0248/83/0000–0000/$03.00

strongly dependent on arsenic acid concentration. Below 0.3M no nucleation occurred in the gel and only a few crystals were obtained above the gel interface.

Solutions of arsenic acid over 1M may inhibit diffusion in the gel by producing a very high nucleation in the interface. To circumvent this problem U tubes were used instead of test tubes; arsenic acid and uranyl nitrate solutions were poured each in a different branch of the tube allowing diffusion of both reactants in the gel, acidified up to pH 1.2 with 20% acetic acid.

For arsenic acid concentrations near 0.5M abundant precipitation also occurred in the interface but after one or two hours small polycrystalline aggregates and well developed plates nucleated in the gel (fig. 1). Both forms competed in the zone from the gel interface to about 4 or 5 cm below it, but further away from the interface isolated plates of about $1 \times 1 \times 0.3$ mm were more frequent.

The two factors that limited the final crystal size in this method are the depletion of the reactants and the increase in the by-product concentration during crystal growth. To avoid the first of these problems, in some of the experiments, we renewed the initial uranyl nitrate solution in the test tubes. Only a slight improvement was noticed: the ultimate size of some of the crystals was about $2 \times 2 \times 0.5$ mm.

One advantage of the gel method is that it is particularly well suited to grow single crystals both above and below T_0, the transition temperature. When the crystals so obtained were cooled below T_0, it was possible to compare the resultant domain structures. Chosen growth temperatures (T_g) were 23 and 40°C. At this last temperature, two different procedures were followed: (a) the crystals were taken out of the gel while they were still at 40°C, that is before going through the transition; for these crystals $T_g = 40$°C; (b) the grown crystals were left to cool down to room temperature (23°C) in the gel, and kept in the gel at this temprature for several days. To stress the point that crystals grown with this procedure suffered a change of temperature during the growth period, from now on their growth temperature will be indicated as $T_g = 40/23$°C.

Best results were obtained in all the cases

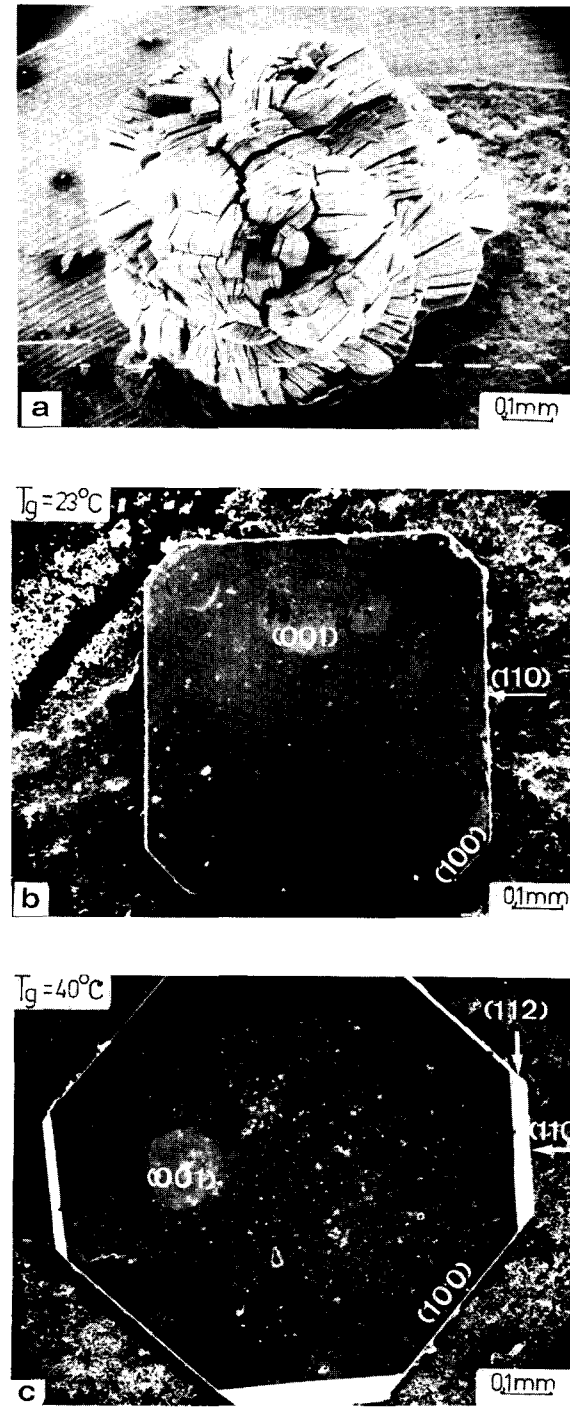

Fig. 1. SEM micrographs of as-grown crystals of HUAsH: (a) polycrystalline aggregate; (b), (c) well developed plates grown at $T_g = 23$°C and $T_g = 40$°C, respectively.

working with test and U tubes uder the following conditions:
- TMS concentration 10 vol%;
- arsenic acid solution 0.5M;
- uranyl nitrate solution 0.5M;
- total time allowed for growth was about 30–40 days.

3. Experimental results

The crystals were identified using X-ray powder diffraction patterns. At room temperature precession patterns of the monoclinic crystals failed to show any departure from tetragonal symmetry.

Three types of thick plates were obtained: type I, with well developed (001) faces which gave a perfect reflection in the optical goniometer, type II with a single growth hillock appearing at the centre of the plates, where four symmetric sectors originate, and type III, with one or two off-centred hillocks present (fig. 2). Most of the crystals obtained belong to type II.

In the optical goniometer, reflections due to the hillock faces (type II and III plates) showed perfect tetragonal symmetry around the tetragonal axis and their normal formed a 20 minute angle with it. The morphology of the crystals changed slightly with the growth temperature. This was particularly noticeable in the different development of the (*hh*0) and (*hhl*) faces (fig. 1).

The layered crystalline structure of HUAsH is responsible for the perfect cleavage on (001). This cleavage is evident in the scanning electron micrographs of the carbon–gold coated HUAsH platelets (fig. 3a). These cleavages were produced under the electron beam of the SEM and are probably due to local stresses generated by non-homogeneous heating of the sample, particularly when working under high magnification. When the sample was kept for several hours under observation, dehydration started, as seen in fig. 3b).

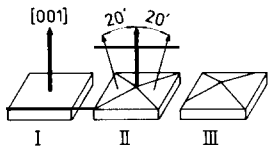

Fig. 2. Different types of plates. Schematic drawings: (I) (001) plate; (II) plate with single central growth hillock; (III) plate with off-centred hillock.

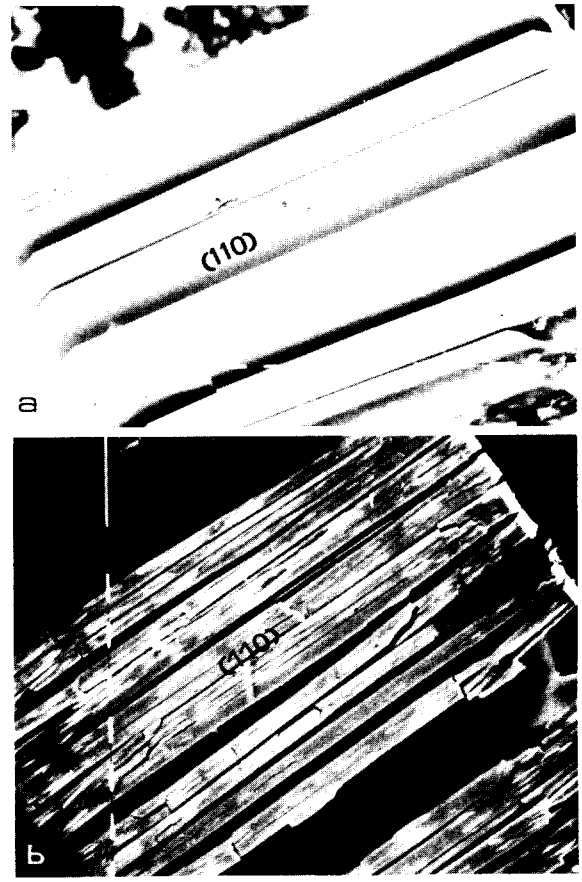

Fig. 3. (a) (001) cleavage traces on (110) face; (b) same crystal after dehydration under the electron beam.

4. Domain structure

Crystals obtained by the gel method have a paraelastic–ferroelastic transition temperature (T_0) between 26 and 28°C which is quite similar to the highest transition temperature observed in crystals grown from solution [1].

This phase transition is detected optically on the (001) face by the observation of domains at 90°, with domain walls running nearly parallel to [110] and [1$\bar{1}$0] directions of the tetragonal phase (fig. 4).

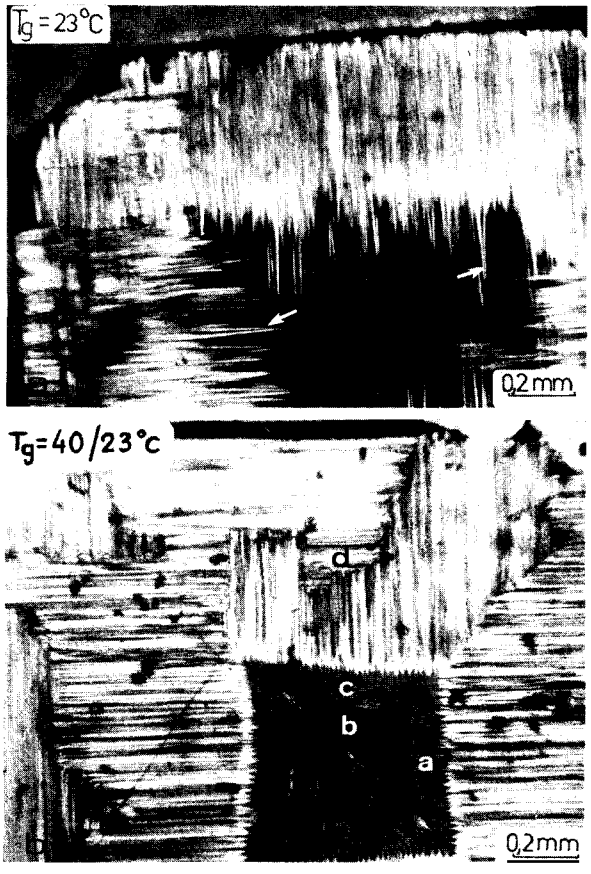

Fig. 4. Domain structure observed on (001). Optical micrographs taken between crossed polarizers: (a) as-grown crystal (T_g = 23°C); (b) crystal cleaved through the nucleation centre (T_g = 40/23°C).

Domains with domain walls parallel to [100] can be detected only with oblique illumination [1] and they were also observed in gel-grown crystals. Fig. 5 shows a very small crystal, still immersed in the gel matrix and showing a simple domain structure in which both types of domains are present. Domain structures of both solution grown and gel-grown crystals are identical. Crystals grown at $T_g < T_0$ and crystals which have undergone several phase transitions show a fine grid-type array of many small thin domains and in most of these crystals a superposition of two slightly rotated arrays (I and II) of the 90° domains appear (figs. 4a and 4b). This is particularly clear when thin

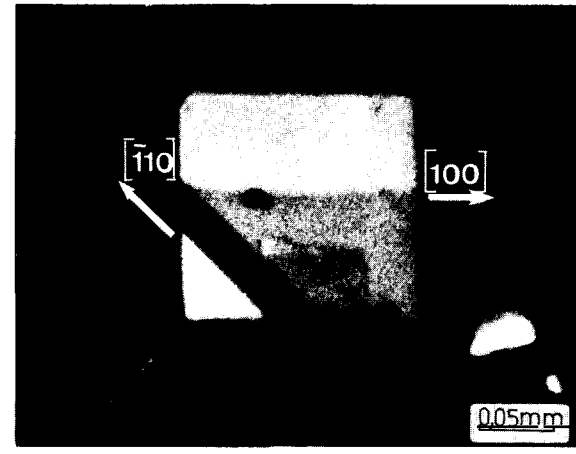

Fig. 5. Small crystal immersed in the gell matrix, showing domain walls parallel to [110] and [100].

cleavage slices are observed in the optical microscope. With white light, perpendicular incidence, crossed polarizers and a $\frac{1}{4}\lambda$ plate, nearly parallel domains in sets I and II show different optical orientations: when domains in set I appear blue, those in set II appear yellow (fig. 6a). In most crystals these slightly rotated domains seem to have a common origin, although sometimes they run parallel for short distances before diverging (fig. 6b). A typical example is indicated by arrows in fig. 4a. These rotated domains are similar to the twisted structure mentioned by Benyacar and de Abeledo [1] in solution grown crystals. We have not yet found a plausible explanation for the pres-

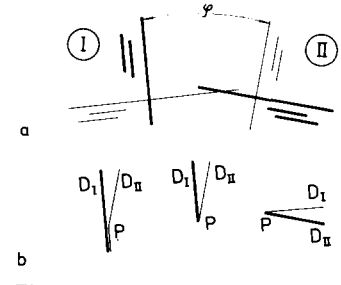

Fig. 6. Schematic drawing of I and II arrays of 90° domains. Thick lines indicate blue colour; thin lines indicate yellow colour. (a) φ rotation angle between I and II sets. (b) Interaction between nearly parallel domains belonging to different sets; (P) apparent common origin.

ence of these two sets of domains.

Crystals grown at $T_g > T_0$ and slowly cooled in the gel, when observed under the same conditions, show only a few broad domains oriented preferentially along only one of the two ⟨110⟩ tetragonal directions. The thick crystals obtained by the gel method allowed us to gather new information on the three-dimensional characteristics of the domain structure. Although it has not been possible to obtain thin sections parallel to the tetragonal axis due to the very easy and perfect cleavage parallel to (001), optical observations were carried out on (100) and (110) lateral faces of the as-grown crystals ($T_g = 40/23$°C).

In transmitted light and crossed polarizers two sets of birefringent zones of variable width forming an angle with the c tetragonal axis and sometimes interacting with one another were observed. A few bands or walls parallel to the c axis were also present. These bands should be related to domains which were observed on the (001) face of the samples studied under the same conditions because they disappeared when the sample was heated above the transition temperature and they could also be observed at $T < T_0$ in the interior of the crystal through a change of focus.

A slightly more complex structure was observed when the lateral surfaces of the crystal were studied with asymmetrically diaphragmed illumination in order to enhance the contrast of the bands; interaction between bands was here clearly visible (figs. 7a and 7b). When the sample was heated above T_0,

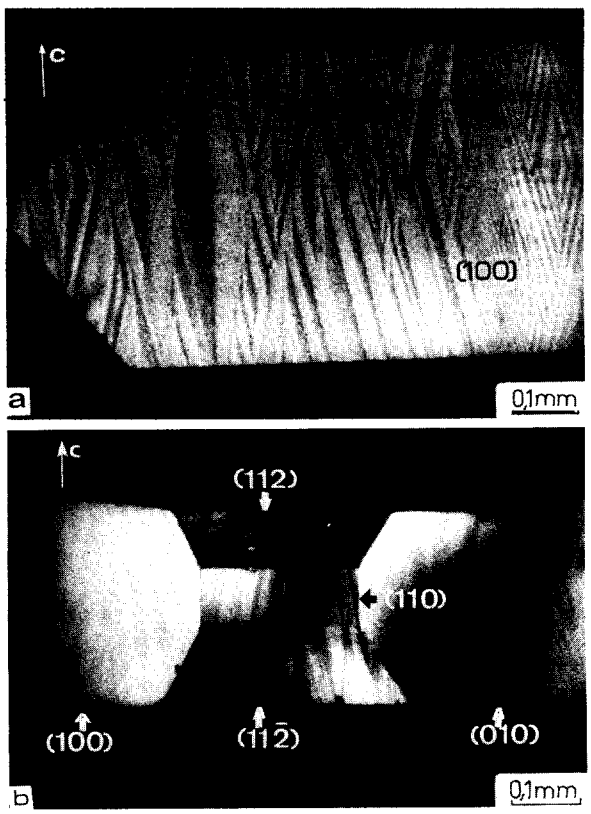

Fig. 7. Transmission optical micrographs of as-grown crystals ($T_g = 40/23$°C) taken with asymmetrically diaphragmed illumination: (a) (100) face; (b) traces of domains crossing several lateral faces.

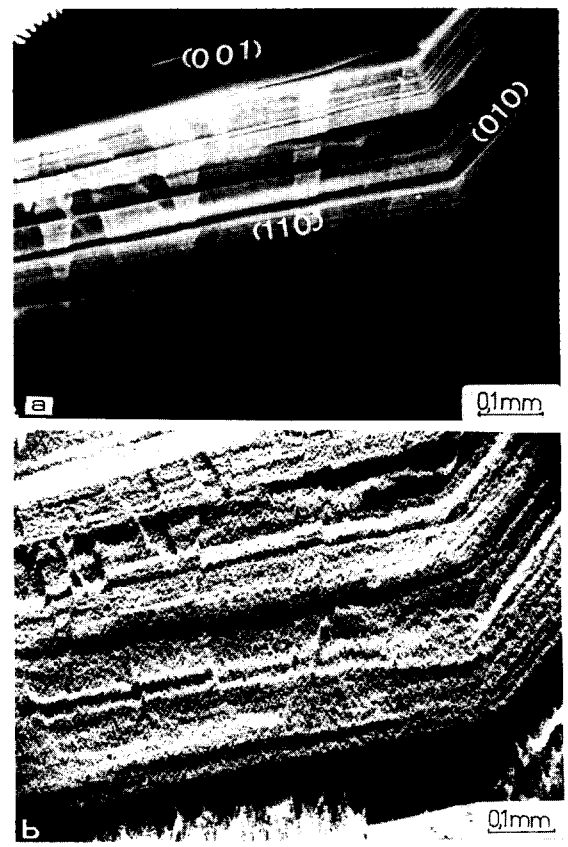

Fig. 8. SEM micrographs of as-grown crystals ($T_g = 40/23$°C): (a) secondary electron image 25 kV; (b) the same area displayed with Y modulation mode.

not all of these traces disappeared; the remaining ones can be related to surface relief. To prove this, scanning electron micrographs were taken (figs. 8a and 8b). The relief was particularly remarkable when the secondary electron mode with Y modulation was used (fig. 8b).

We must recall that these crystals initially grown at $T_g > T_0$ were left to cool in the gel and were kept in the gel at room temperature for several days; during this stage the crystals continued to grow in the ferroelastic phase in which domains are present. The relief observed on $\{hk0\}$ and $\{hhl\}$ faces could be explained by a difference in the growth rates of neighbouring domains which have different crystallographic orientations. Besides, these surface structures are always present in the crystals grown at $T_g < T_0$; but they are absent in crystals grown at 40°C, which were never allowed to go through the transition during the growth stage.

It can be concluded that domains (and domain walls) are responsible for both birefrigent zones and relief observed on $\{hk0\}$ and $\{hkl\}$ faces.

5. Growth history

It has been stressed [10] that in the case of crystals grown by flux and solution methods a variety of growth features exist even in different specimens from the same experiment. The generalization on growth mechanisms for crystals obtained by these techniques should then be expressed with care.

This is also true in the conventional gel growth experiments; the gel is not in a stationary steady state because of changes in the reactant concentration along the length of the tube and as a function of time. The local conditions around each growing crystal are not well defined and it is not possible to generalize any growth mechanism.

Nevertheless some qualitative information about growth history and crystal perfection may be inferred in the case of gel-grown HUAsH, from defects revealed by chemical etching and from domain structures developed both in as-grown specimens and cleaved slices.

6. Growth history and crystal perfection

When typical gel-grown crystals (type I and II) were observed in the optical microscope at $T > T_0$ (tetragonal phase) they showed homogeneous extinction and no visible inclusions.

In a few type III crystals, extinction was not homogeneous: the strained zone shown in fig. 9 coincides with the off-centred hillock and is probably related to the presence of localized defects. Interaction of close, parallel dislocations of like-sign originating at the core of the crystal may be responsible for the polygonal growth spirals observed in the optical microscope on the as-grown (001) surface of some type I crystals; similar spirals were observed in other materials [10,11]. To check the distribution of imperfections inside the crystals, cleavage slices cut as shown in fig. 10b were etched 1 min with a 10% aqueous nitric acid solution at room temperature. The slice (L_1) intersecting the core of a typical type II crystal ($T_g = 40/23$°C) showed remarkable inhomogeneity in the distribution of square etch pits; they were preferentially located in a central nearly square zone (N) (fig. 11a). Outside this zone only a few pits developed.

Fig. 11b shows a pair of matching cleavage surfaces (zone C, centre of N); the etch patterns originate from a pair of screw dislocations of opposite sign which are related to the top of the

Fig. 9. Type III crystal. Non-homogeneous extinction and preferential generation of domains observed in the strained zone below the off-centred hillock.

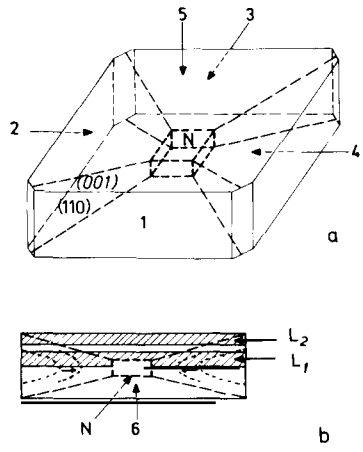

central hillock observed on the (001) face of these crystals. Similar interrelation between hillocks and dislocated regions have been reported in other layered structures (such as graphite) and in refractory oxide crystals [10]. Etch pits are always observed in zones of "poor growth". They can

Fig. 10. Schematic drawing of growth sectors for crystals grown at $T_0 = 23°C$: (a) (N) central zone corresponding to the initial stages of growth; (1–4) {110} sectors; (5), (6) {001} sectors. (b) Growth sectors projection on (110); arrows indicate birefringent zones advancing with decreasing temperature when the crystal is observed between crossed polarizers ($T < T_0$); (L_1), (L_2) cleavage slabs.

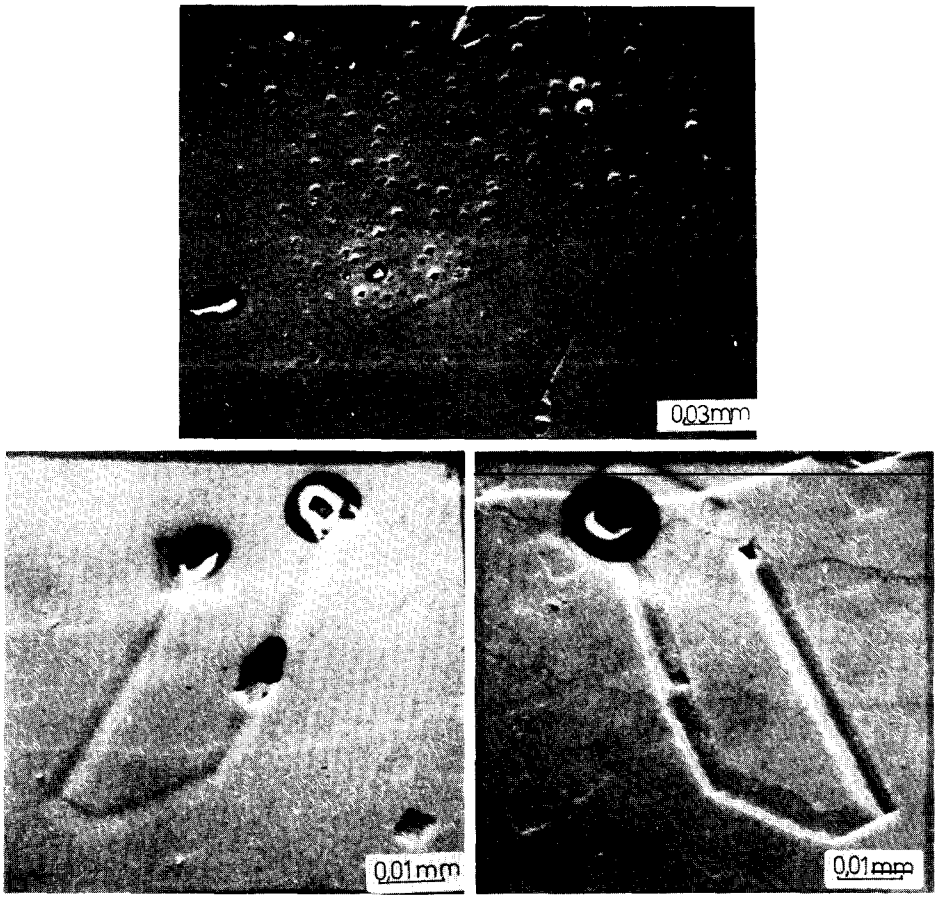

Fig. 11. (001) cleaved slab (L_1) of a typical type II crystal: (a) Etch pits localized in the central zone (N) (centre (C) of (N) out of the field of view; only one fourth of zone (N) is shown). (b) Zone (C); etch pattern of a pair of screw dislocations on (001) matching cleavage surfaces through the nucleation centre.

originate from etching both at point defects and at dislocations formed in the rapid initial stages of growth; the deep pits that were observed are most probably associated with the outcrop of dislocations. Besides, in some crystals a slight difference in pit density is found around the diagonals of the zone (N) delineating a petal-like figure.

The observations suggest the following sequence of growth stages:

(1) An initial rapid dentritic growth. This assumption is supported by the features revealed in fig. 12. It shows a very small crystal which grew on the tube wall; a petal-like figure reveals the imprint left in the gel by the dentritic crystal, which latter grew and suffered different perturbations (partial dissolution and recrystallization) until the final square shape was achieved. Gel cusp-like cavities similar to those mentioned by Henish [6] and indicated by arrows in fig. 12 are observed, generally associated with the corners of most of the HUAsH crystals still immersed in the gel; they are filled with nitric acid containing solution which is responsible for the partial dissolution process.

(2) A more stable "further growth" stage, revealed by the absence of etch pits at the outer zone of the crystal; the neat outline of (N) is the boundary between both zones and reveals the shape of the crystal when stable growth started.

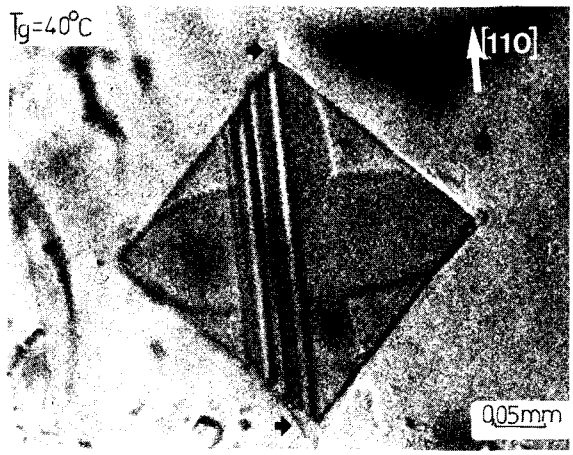

Fig. 12. Small crystal immersed in the gel. Petal-like imprint left in the gel by the initial dentritic crystal. Black arrows indicate the cusp-like gel cavities at the corners of the final square crystal.

7. Growth history and domain structure

We must recall that ferroelastic domains are quite sensitive to stresses, whichever their origin; external applied stresses, mechanical damage, internal stresses associated with the presence of sector boundaries and growth defects, all of them influence domain nucleation and growth, so growth history may be inferred also from the generation, growth and distribution of ferroelastic domains.

In crystals grown at $T_g = 23°C$, the domains observed on (001) at T slightly below T_0 (see fig. 4a), are preferentially oriented in the four sectors $\{110\}$; they originate at the crystal edges and propagate along [110] or $[1\bar{1}0]$ towards the centre of the face. If the crystal is observed standing on (110) between crossed polarizers at the extinction position, birefringent zones appear at the transition temperature at the crystal edges, advancing towards the core. The "transition fronts" roughly delineate an "hour glass" contour as shown by broken lines in fig. 10b.

On lowering the temperature further, birefringence appears throughout the crystal.

So, the core and the $\{001\}$ sectors have a slightly lower transition temperature ($\Delta T_0 = 1°C$) than the four $\{110\}$ sectors (see fig. 10a).

To check this, the uppermost cleaved (L_2) slice, which cuts mostly through the $\{001\}$ sector, was studied. It did not show an inhomogeneous domain distribution: domains appear simultaneously at $T = T_0$ throughout the cleaved slice.

Similar behaviour is generally observed in a crystal grown at $T_g = 40/23°C$, notwithstanding the fact that some additional features are present in a slab cutting through the nucleation centre (fig. 4b). Four different zones (a, b, c and d) are present in this figure, which can be related to growth bands, involving stress-inducing impurity segregation [12,13]; growth bands arising from local variations of the impurity content can show slightly different transition temperature T_0. This could be the origin of the differences observed between zone c (no domains are yet present) and neighbouring zones b and d which have already gone through the transition.

These zones are outlined by the domain tips and show the sequential contours of the growing

crystal. Anisotropic strains are present in zone a, and as we have shown in fig. 11b, they are related to the presence of dislocations. Apex perturbations, clearly visible in the outline of zones b and c are indicative of growth instabilities at the early stage of growth [14]. Later, well developed faces formed as the crystal grew under more stable growth conditions.

The same sequence was concluded from chemically etched samples, where the outer zone of the crystal showed only a few grow-in dislocations.

8. Conclusions

HUAsH crystals, grown from gelled solutions of 10% TMS at different temperatures, allowed us to study the three-dimensional characteristics of domain walls present in the monoclinic phase. We have shown that there are three types of domain walls: one parallel to the tetragonal c axis and two symmetrically inclined to it.

Growth history has been inferred from chemical etching of defects and domain structure observations. Etch pits developed in cleaved slices show that screw dislocations play an important role in the nucleation and growth of crystals.

In this ferroelastic material the transition temperature seems to be quite sensitive to the presence of stresses and slight differences in composition.

Selective trapping of impurities in different growth-sectors and impurity segregation in growth bands must be responsible for the characteristic domain nucleation and further growth observed on (110), (100) and (001) facets.

We think that the assessment of crystal quality and the correlation between optical observations of domain structures and growth defects in gel grown crystal of HUAsH could be more precisely established if X-ray topographs could be taken above and below the paraelastic–ferroelastic transition temperature, T_0.

Acknowledgements

The authors thank Dr. María A.R. de Benyacar for her fruitful collaboration on the research described in this paper and Dr. Patricia Perazzo for her help with the X-ray work.

References

[1] M.A.R. de Benyacar and M.E.J. de Abeledo, Am. Mineralogist 59 (1974) 763.
[2] M.E. Mrose, Am. Mineralogist 38 (1963) 1159.
[3] M.A.R. de Benyacar and H.L. Dussel, Ferroelectrics 9 (1975) 241.
[4] M.A.R. de Benyacar and H.L. Dussel, Ferroelectrics 17 (1978) 469.
[5] H.L. de Dussel, L.S. de Wainer and M.A.R. de Benyacar, Ferroelectrics 46 (1982) 25.
[6] H.K. Henisch, Crystal Growth in Gels (Pennsylvania Univ. Press, 1968).
[7] S.K. Arora, Progr. Crystal Growth Characterization 4 (1981) 345.
[8] F. Lefaucheux, M.C. Robert, E. Manghi and H. Arend, J. Crystal Growth 51 (1981) 551.
[9] H. Arend and J.J. Connelly, J. Crystal Growth 56 (1982) 642.
[10] H.J. Scheel and D. Elwell, J. Crystal Growth 20 (1973) 259.
[11] A.R. Verma, Crystal Growth and Dislocations (Butterworths, London, 1953).
[12] A. Authier, in: Current Topics in Material Science, Vol. 2, Ed. E. Kaldis (North-Holland, Amsterdam, 1977) p. 516.
[13] H. Klapper, paper presented at Characterization of Crystal Growth Defects by X-Ray Methods, Durham, UK, 1979.
[14] A.A. Chernov, J. Crystal Growth 24/25 (1974) 11.